Author Manuscript

Author Manuscript

Author Manuscript

Author Manuscript

HHS Public Access

Author manuscript

Neurobiol Dis. Author manuscript; available in PMC 2021 October 01.

Published in final edited form as:

Neurobiol Dis. 2021 October ; 158: 105486. doi:10.1016/j.nbd.2021.105486.

Altered synaptic glutamate homeostasis contributes to cognitive decline in young APP/PSEN1 mice

J.M. Wilcox[a,b], **D.C. Consoli**[a], **A.A. Tienda**[b], **S. Dixit**[b,1], **R.A. Buchanan**[a], **J.M. May**[b], **W. P. Nobis**[c,2], **F.E. Harrison**[b,*,2]

[a] Program in Neuroscience, Vanderbilt University, Nashville, TN, United States of America

[b] Department of Medicine, Vanderbilt University Medical Center, Nashville, TN, United States of America

[c] Department of Neurology, Vanderbilt University Medical Center, Nashville, TN, United States of America

Abstract

Non-convulsive epileptiform activity is a common and under-studied comorbidity of Alzheimer's disease that may significantly contribute to onset of clinical symptoms independently of other neuropathological features such as β-amyloid deposition. We used repeated treatment with low dose kainic acid (KA) to trigger subthreshold epileptiform activity in young (less than 6 months) wild-type (WT) and APP/PSEN1 mice to test the role of disruption to the glutamatergic system in epileptiform activity changes and the development of memory deficits. Short-term repeated low-dose KA (five daily treatments with 5 mg/kg, IP) impaired long-term potentiation in hippocampus of APP/PSEN1 but not WT mice. Long-term repeated low-dose KA (fourteen weeks of bi-weekly treatment with 7.5–10 mg/kg) led to high mortality in APP/PSEN1 mice. KA treatment also impaired memory retention in the APP/PSEN1 mice in a Morris water maze task under cognitively challenging reversal learning conditions where the platform was moved to a new location. Four weeks of bi-weekly treatment with 5 mg/kg KA also increased abnormal spike activity in APP/PSEN1 and not WT mice but did not impact sleep/wake behavioral states. These findings suggest that hyperexcitability in Alzheimer's disease may indeed be an early contributor to cognitive decline that is independent of heavy β-amyloid-plaque load, which is absent in APP/PSEN1 mice under 6 months of age.

Keywords

Alzheimer's disease; Glutamate; Memory; Behavior; Mouse; EEG; Electrophysiology

This is an open access article under the CC BY-NC-ND license (http://creativecommons.org/licenses/by-nc-nd/4.0/).

* Corresponding author. fiona.harrison@vumc.org (F.E. Harrison).

[1] Affiliation at time work was conducted.

[2] These authors contributed equally to the manuscript and will be co-corresponding authors

Declaration of Competing Interest

None.

Appendix A. Supplementary data

Supplementary data to this article can be found online at https://doi.org/10.1016/j.nbd.2021.105486.

Author Manuscript Author Manuscript Author Manuscript Author Manuscript

1. Introduction

Alzheimer's disease (AD) is the most common form of dementia and a significant public health problem for which there is currently no effective long-term treatment. Recent evidence suggests that non-convulsive epileptiform activity is a common and under-studied comorbidity of AD, (Horvath et al., 2016; Horvath et al., 2018; Vossel et al., 2013; Vossel et al., 2016; Vossel et al., 2017) a phenomenon that has been recognized for several decades (Volicer et al., 1995). Subclinical changes in hyperexcitability may begin years or even decades prior to the earliest signs of cognitive decline. New data suggest that subclinical epileptiform changes are more common than previously believed (Cretin et al., 2017b; Vossel et al., 2016). Importantly, unprovoked seizures and subclinical epileptiform activity were reported at prodromal stages of AD, starting in some cases long before both clinical symptoms and alterations in brain imaging, suggesting a role for this process in the early pathogenesis of AD. A diagnosis of childhood onset epilepsy was associated with greater Aβ burden five decades later compared to a control population (Joutsa et al., 2017). These data suggest that abnormal neuronal activity may contribute directly to development of AD neuropathology including Aβ accumulation. The extent to which these abnormal brain electrical discharges may drive cognitive decline directly (Chin and Scharfman, 2013; Lam et al., 2017) or indirectly through interactions with AD neuropathology is currently unknown.

Findings of abnormal hyperexcitability and seizures have been replicated in several mouse models of AD (Gureviciene et al., 2019; Gurevicius et al., 2013; Minkeviciene et al., 2009; Palop et al., 2007; Roberson et al., 2011; Ziyatdinova et al., 2016) including data from our own group showing that even a single, mild pharmacologically-induced seizure following a low dose of kainic acid can lead to memory deficits in young APP/PSEN1 mice (Mi et al., 2018). Increased extracellular glutamate in epileptogenic compared to non-epileptogenic tissue was reported in both hippocampus and cortex in epilepsy patients as measured by in vivo microdialysis (Cavus et al., 2005). Age-dependent changes in glutamate release were reported in APP/PSEN1 mice (Minkeviciene et al., 2008). The data support a role for increased glutamate release or impaired clearance, including slowing of the glutamate-glutamine recycling system playing a key role in epileptogenesis in this model. The excitatory amino acid transporters GLT-1 and GLAST (EAAT2 and EAAT1) are membrane bound trimeric proteins responsible for the majority of glutamate clearance in cortical and hippocampal areas. Estimates vary regarding relative expression and functional role in synaptic glutamate clearance but it is estimated that up to 90% of GLT-1 protein is localized to astrocytes, with just 10% localized to neuronal membranes (Petr et al., 2015). Together it is estimated that up to 95% of synaptic glutamate is cleared by GLT-1 (Danbolt et al., 1992; Tanaka et al., 1997). Altered expression or function of either of these transporters are associated with a wide array of degenerative and neuropsychiatric disorders (Pajarillo et al., 2019; Petr et al., 2015; Tanaka et al., 1997). A de novo genetic mutation (single nucleotide polymorphisms, SNPs) in GLAST that decreased glutamate uptake was associated with seizures and other neurological deficits (Jen et al., 2005). Heterozygous deletion of GLT-1 accelerated cognitive decline in a water maze task in middle-aged (6–9 months) APP/PSEN1 transgenic mice (Mookherjee et al., 2011). Interestingly, deletion of

Author Manuscript Author Manuscript Author Manuscript Author Manuscript

astrocytic versus neuronal GLT-1 in mice led to a different cognitive profile of deficits and was also associated with differences in synaptic and neuroinflammatory regulation (Sharma et al., 2019). Neuronal GLT-1 may be more directly involved in mitochondrial energetics (McNair et al., 2019). In contrast, overexpression of GLT-1 in an alternate mouse model of AD ($APP_{Swe,Ind}$) was protective against spontaneous mortality in mice less than 4 months old, and in three tests of cognitive function in 12–14 month old animals (Takahashi et al., 2015). These data suggest that modulation of glutamate clearance at the synapse plays a vital role in protection against AD-like cognitive deficits, and that this may be at least partially mediated by epileptic activity. It is possible that early prevention or suppression of chronic subclinical epileptiform activity could be a realistic strategy to minimize cognition decline trajectories in AD patients, whether or not this also impacts underlying AD-specific pathology (Cretin et al., 2017a).

Seizures trigger a cascade of damage to hippocampal circuitry to ultimately impact learning and memory. Similar synaptic damage can manifest through chronic exposure to Aβ and aggregation of hyperphosphorylated tau. Such disruption of normal brain circuit function may be impacted by increased excitability or decreased suppression via inhibitory circuits. In the present study we used a repeated-dose treatment strategy to increase hyperexcitability via low concentrations of the glutamatergic kainite receptor agonist kainic acid (KA). We used young APP/PSEN1 mice from 12 to 14 weeks of age, prior to deposition of Aβ plaques, to investigate the hypothesis that hyperexcitability caused by repeated dosing of low KA would disrupt long term potentiation (LTP), impair complex learning and memory tasks, and that this would be detectable as an increase in abnormal EEG activity even during early stages of AD pathology and in the absence of overt seizures.

2. Methods

2.1. Animals and drug treatments

Female C57Bl/6 J wild-type mice (Jackson laboratories strain No. 000664) and male bigenic $APP_{SWE}/PSEN1_{\Delta E9}$ mice (Jackson laboratories strain No. 005864; MMRRC Stock No: 34832) were obtained from Jackson Laboratories and used to found the colonies used in this study. All mice were aged to 12 to 24 weeks as noted for each study, and approximately equal numbers of male and female mice were used. APP/PSEN1 mice develop a small number of Aβ deposits in hippocampus and overlying cortex by 6 months of age, and pathology is typically abundant by 12 months of age. Behavioral deficits are robust at 12 months of age, but deficits may be detectable from 6 months in mice with compounding pathologies (e.g. induced seizures, dietary manipulations (Dixit et al., 2015, Mi et al., 2018)). All animals were housed in a temperature- and humidity-controlled vivarium and were kept on a 12:12 h light cycle. All procedures were approved by the Vanderbilt Institutional Animal Care and Use Committee.

Kainic acid (KA; SigmaAldrich Cat. #K0250) was made up in 0.9% physiological saline and administered at 5–10 mg/kg with an administration volume of 10 ml/kg. Treatment schedules are depicted in Figs. 1A, 2A and 3A.

Author Manuscript Author Manuscript Author Manuscript Author Manuscript

2.1.1. Study 1 – long term potentiation (LTP)—Short-term repeated dosing schedule. Twelve-week-old WT and APP/PSEN1 mice of either sex were treated with 5 mg/kg KA (injected IP) or the saline vehicle for 5 consecutive days. LTP studies were conducted on the 5th day and mice were euthanized a minimum of one hour following the final KA injection.

2.1.2. Study 2 – behavior—Long-term repeated dosing schedule. Twelve-week-old WT and APP/PSEN1 mice of either sex were treated with 7.5–10 mg/kg KA (IP) or the saline vehicle twice per week for up to 8 weeks (maximum of 16 injections). The first 3 cohorts of mice that were tested received 10 mg/kg of KA which led to extremely high death rate in APP/PSEN1 mice (11/14 KA-treated APP/PSEN1 mice died over the course of the experiment, compared to 1/9 saline-treated APP/PSEN1; 0 WT animals of either group died). Therefore, for the final cohort of animals the dose was decreased to 7.5 mg/kg which led to a death rate of 1/4 KA-treated APP/PSEN1 mice. All surviving mice were euthanized following behavioral testing at approximately 20 weeks of age.

2.1.3. Study 3 – EEG, behavior, glutamatergic protein expression and histology—Long-term repeated dosing schedule. Fourteen-week-old WT and APP/PSEN1 mice of either sex underwent surgical implantation of telemetry devices followed by a recovery period of up to 2 weeks. Following surgery mice were single housed to limit cage-mate interference with the surgical site. KA (5 mg/kg, IP) or the vehicle saline were administered twice per week for 5 weeks (10 injections total). Mice were briefly anesthetized with isoflurane to permit delivery of the drug without risk of dislodging EEG recording wires during immobilization.

For all three studies, mouse groups are designated by abbreviations for genotype (WT or APP/PSEN1) and treatment (saline, SAL or kainic acid, KA) to generate four groups for each of the experiments (WT-SAL, APP/PSEN1-SAL, WT-KA, APP/PSEN1-KA) regardless of which treatment schedule was used.

2.2. Long term potentiation (Study 1)

Acute hippocampal slices were prepared from 12-week-old WT and APP/PSEN1 of either sex injected with saline or KA for 5 days with the final dose given within 2 h of euthanasia. Mice under isoflurane anesthesia were transcardially perfused with ice-cold sucrose-rich slicing artificial cerebrospinal fluid (aCSF) containing 85 mM NaCl, 2.5 mM KCl, 1.25 mM NaH2PO4, 25 mM NaHCO3, 75 mM sucrose, 25 mM glucose, 10 uM DL-APV (NMDA antagonist), 100 uM kynurenate, 0.5 mM Na L-ascorbate, 0.5 mM CaCl2, and 4 mM MgCl2, and oxygenated and equilibrated with 95%O2/5% CO2. Following perfusion, mice were quickly decapitated and horizontal brain slices (300 mm) were prepared using a Leica VT-1200S vibratome (Leica Biosystems) in sucrose-ACSF. Slices were transferred to a holding chamber containing sucrose-ACSF warmed to 30 °C and slowly returned to room temperature over the course of 15–30 min. Slices were then transferred to oxygenated ACSF at room temperature containing 125 mM NaCl, 2.4 mM KCl, 1.2 mM NaH2PO4, 25 mM NaHCO3, 25 mM glucose, 2 mM CaCl2, and 1 mM MgCl2 and maintained under these

Author Manuscript Author Manuscript Author Manuscript Author Manuscript

incubation conditions until recording in a submerged chamber (Scientifica SliceScope Pro 2000, Scientific UK).

Field excitatory postsynaptic potentials (fEPSPs) from the Cornu ammonis 1 (CA1) region of the hippocampus were recorded by stimulating the Schaffer collaterals in the stratum radiatum and recording the response with an electrode in the stratum radiatum with responses recorded at a rate of 0.05 Hz. An input-output relationship was determined for each slice, plotting the peak amplitude of the fiber volley against the slope of the fEPSP. For LTP experiments, the baseline recordings used a stimulus intensity that produced ~40% of the maximum response and were recorded for at least 20 min before tetanizing the slice. LTP was induced using a high intensity theta-burst stimulation (four bursts each at 100 Hz, with these bursts repeated at 5 Hz over 5 s, with each tetanus including ten of these burst trains separated by 15 s). Experiments in which the fiber volley amplitude changed by >20% post-tetanus were discarded. Recordings were continued for at least 60 mins post-tetanus. The magnitude of LTP was measured at time a point between 50 and 60 min post tetanus, whereas post-tetanic period was measured at 1–5 min after the tetanus. There were 7–8 slices from each group from 3 to 4 mice.

2.3. Behavioral testing (Studies 2 and 3)

All behavioral testing was undertaken using facilities of the Vanderbilt Murine Neurobehavioral Laboratory Core facility. If testing occurred on a day on which treatment was administered, then the injection was given after behavioral testing was completed to avoid confounding of data by the acute effects of the drug.

2.3.1. Elevated zero maze (Studies 2 and 3)—Anxiety was measured using a standard white Elevated Zero Maze (San Diego Instruments, CA). The maze consists of a circular platform (~6-cm width with a ~ 40-cm inner diameter) that is equally divided into four quadrants. Two quadrants on opposite sides of the platform are enclosed by walls (~20 cm high); the other two quadrants are open and bordered by a lip (~0.6 cm high). The maze is elevated 75 cm above the floor. Open zone lighting ranged 461–470 LUX and closed arms 206–256 LUX). A single 5-min trial was recorded using a camera suspended from the ceiling above the maze, and exploration paths in open and closed zones were analyzed for distance traveled and time spent in each zone of the maze using AnyMaze (Stoelting Co. IL). An experimenter monitored the trial remotely from an adjacent room.

2.3.2. Locomotor activity (Studies 2 and 3)—Activity was measured using standard locomotor activity chambers (approx. 30 × 30 cm, ENV-510; MED Associates, Georgia, VT, USA). The walls of the chamber are transparent except for the infrared beam detector which is approximately 2 cm high from the floor. Each chamber is housed within a closed sound attenuating chamber to restrict view of the room or other mice during testing. Activity was recorded automatically for 30 min (Study 2) or 60 min (Study 3) via the breaking of infrared beams.

2.3.3. 2-trial Y maze (Study 2)—Short term memory and spatial discrimination in the Y-maze was assessed as preference for exploring a previously blocked arm of the maze

Author Manuscript Author Manuscript Author Manuscript Author Manuscript

compared to the two familiar arms. The Y-maze had square arms with straight walls (length 35 cm, height 10 cm) which were open at the top. Specific visual clues were placed next to each arm to help differentiate them (a plastic ball, an empty water bottle, a metal pencil cup) in addition to distal room cues. During the first trial one arm was blocked and mice were allowed to explore the two open arms for 5 min. Following an inter trial interval of approximately 2 min during which time the maze was cleaned with a 10% ethanol solution to mask odor cues the mouse was returned to the maze and permitted to explore for a further 5 min. Trials were recorded using a camera suspended from the ceiling above the maze, and exploration in each arm was analyzed using AnyMaze (Stoelting Co. IL). During testing an experimenter monitored the trial remotely from an adjacent room.

2.3.4. Water maze (Study 2)—Water maze testing was conducted in a 107-cm diameter white pool. The escape platform was a white circular acrylic platform (10 cm diameter) that could be raised or sunk and positioned in different places in the pool using a custom designed insert. Water was maintained at room temperature between 22 and 25 °C. For all training days there were four trials given with approximately 15 mins. Inter trial interval and mice were released from a different location at the pool edge each day. For the first 2 days of testing the platform surface was visible above the water and a marker that was visible to the mice while swimming (a white pole with a black ball at the top covered by a white disk), was inserted into the platform. Additional room cues included a table, sink, door and white screens marked with black tape. The platform was located in a different quadrant in the maze during each of the four daily trials. During hidden platform testing the water was rendered opaque through the addition of non-toxic white paint and the platform was submerged 1 cm below the water surface and remained in the same location throughout all 5 days of testing. Water level was approximately 10 cm below the top of the pool. On the first day of reversal learning the platform was moved to a different quadrant, but then remained in that location for all 3 days of testing. Twenty-four hours following the final hidden platform and reversal learning training trials a 60-s probe trial was conducted during which time the platform was sunk and mice were forced to remain in the pool for the entire trial. For all phases of testing trials lasted a maximum of 60 s. Following each trial mice were permitted to recover in clean cages lined with absorbent paper with half of the floor surface located on a warming pad. Sessions were captured by an overhead camera and swim paths and escape latencies were analyzed using AnyMaze (Stoelting Co. IL). Swim speed and peripheral swimming (time within 10 cm of the pool wall) were also assessed to determine whether differences in performance could be attributed to non-cognitive factors.

2.3.5. Force plate actimeters (Study 2)—Force-plate actimetry (FPA) data were collected and analyzed using FPA analysis software provided by the manufacturer (Basi, USA) (McCarson et al., 2018). Mice administered their final treatment of KA or saline and were immediately placed into the arena. They were permitted to freely explore the arena (42 × 42 cm chamber) for 20 min. During this time, the actimeter recorded several parameters that were used for further analysis including total distance traveled and bouts of low mobility (BLM). BLM were calculated for immobility across 5 s periods in areas with a radius of 15 mm, in 20 s time bins across the 20 min session.

Author Manuscript Author Manuscript Author Manuscript Author Manuscript

2.3.6. Conditioned fear (Study 3)—Fear conditioning was conducted using two specialized chambers and computer software (Med Associates Inc. USA). Mice were placed in conditioning chambers that had a plexiglass door, metal walls and a metal grid floor through which a shock could be delivered. These were housed within sound attenuating chambers. During the initial training trial mice learned to associate a 30 s tone with a 2 s electric shock (0.7 mA). There were three tone-shock pairings during the 8-min trial. Twenty-four hours later mice received a context-retrieval trial in which they were placed in the same testing chamber that was used the day before and left undisturbed for 4 min before being returned to the home cage. One hour later the context was altered by placing a white plastic, curved wall and floor into the chambers, along with a dish containing 1 ml of vanilla extract flavoring (McCormick, USA) just outside the enclosed chamber but within the outer containment box. Following 2 min exploration in the novel context the tone was played for 2 min and freezing response measured. Testing rooms had two ante chambers and so testing context was further altered by varying the entrance room and lighting conditions between the two retrieval trials. For each trial cameras mounted to the inside of the door of the outer containment box and computer software scored the mice for the amount of time spent immobile, reported as time freezing.

2.3.7. Test order—For Study 2 testing was conducted in the following order: *Week 1.* Elevated zero maze, locomotor activity, Y-maze; *Weeks 2–3.* Water maze. *Week 4.* Force plate actimeters and euthanasia. The final KA or saline injection was administered immediately prior to testing with the force plate actimeters, approximately 1–3 h prior to euthanasia.

For Study 3, after four weeks of EEG recording, behavioral testing was conducted in the following order and completed in one week: Elevated zero maze, locomotor activity, fear conditioning, and final KA or saline injection approximately 1–3 h prior to euthanasia.

2.4. In vivo electrophysiology (Study 3)

2.4.1. Telemetry device implantation—Under sterile technique, a wireless telemetry device (PhysioTel HD-X02; Data Sciences International, DSI, St. Paul, MN) was implanted subcutaneously following DSI-approved protocol in mice between 14 and 16 weeks of age. Isoflurane was used to induce (2–5%) and maintain appropriate anesthesia throughout the procedure. Mice were secured in a stereotaxic instrument via ear bars and a scalpel was used to expose the skull and neck muscles. From here, rounded surgical scissors were used to create a subcutaneous pocket on the left side of the body. The device was placed in this pocket so that it was positioned between the left shoulder and left hip, with minimal to no impediment to movement. Recording and reference electromyograph (EMG) wires (0.3 mm diameter helix of stainless-steel coils protected with silastic coating 0.63 mm in diameter), were placed in the neck muscle. For placement of the electroencephalograph (EEG) wires, two 1-mm burr holes (from bregma +1.5 mm anterior-posterior and − 1.5 mm medial-lateral for reference; − 1.5 mm anterior-posterior and +1.5 mm medial-lateral for recording) were created using a hand drill. One of two DSI-approved methods was used for placement of the EEG leads, either 1) the indirect method, in which a lead was wrapped twice around a 1.1-mm stainless steel screw that was inserted into each burr hole, or 2) the direct method,

Author Manuscript Author Manuscript Author Manuscript Author Manuscript

which omitted the use of skull screws and the lead was inserted directly into the burr hole such that the coils of the lead secured its position against the perimeter of the burr hole. Regardless of EEG lead placement method, the skull was covered with dental cement and the incision site sutured. The indirect method was used for the first two cohorts ($n = 14$), but the direct method was used on the remaining animals ($n = 15$) to improve animal welfare and promote healing at the suture site as a result of reduced bulk under the dental cement. Lead placement method does not impact data acquisition. Analgesic (ketoprofen, 10 mg/kg, IP) was administered immediately following surgery and every 24 h for 48 h. After surgery and for the remainder of the study, mice were singly housed to avoid disruption of the implanted device and surgical site.

2.4.2. Electroencephalogram (EEG) data acquisition—Electrophysiological data were collected using Ponemah Physiology Platform version 5.20 software (DSI, St. Paul, MN). Each singly housed mouse remained in its home cage placed on a PhysioTel receiver plate (model RPC-1) that transmitted data in real time from the wireless implant to a computer using the MX2 data exchange matrix Dataquest ART software (DSI, St. Paul, MN). Single channel EEG and EMG were continuously sampled at a rate of 500 Hz. Core-body temperature and activity measures were sampled at 50 Hz. High definition (20–30 frames/s) video of each mouse, synchronized to its physiologic measurements, was recorded using Axis cameras (M1145-L) and MediaRecorder 2.6 (Noldus). EEG recording began within 2 weeks of surgery. Approximately 72 h of continuous data were collected each week for four consecutive weeks. KA injections (5 mg/kg) were administered IP twice weekly throughout the recording period (Tuesday/Friday between 11:00 and 16:00). Mice were briefly anesthetized with isoflurane prior to injections to avoid displacing the EMG and EEG leads during handling. One of the two weekly injections occurred during physiologic data collection and mice were removed from the receiver plate for less than 5 min.

2.4.3. EEG data analysis—NeuroScore version 3.3.0 (DSI, St. Paul, MN) was used to perform data analysis. EEG was recorded 24 h prior to the first injection and a two-hour section of data immediately prior to the first injection was analyzed to determine spiking activity at baseline. Baseline data were lost for $n = 10$ of 30 animals due to an unfortunate computer shutdown and auto-update which was subsequently disabled. The two hours immediately following KA or saline injection during weeks 1 and 4 were analyzed to examine how the acute effects of KA changed over repeated activation of the glutamatergic system. First, spikes and spike trains were detected using the NeuroScore automated seizure detection software with the following parameters: spikes were at least 200 uV in amplitude (no greater than 5000 uV) and at least 1 ms long (no greater than 70 ms). Spike trains had a minimum spike interval of 0.05 s and maximum spike interval of 1 s; minimum train duration 0.5 s, train join interval of 1 s and minimum number of spikes per train was 3 (Losing et al., 2017)). All EEG data were processed with a 1 Hz high pass filter. Automated scoring was validated by a blinded investigator to remove signal artifacts or dropouts (Supplemental Fig. 1) and to confirm characteristic EEG spikes associated with a head bob (visualized via synchronized video). Spikes and spike trains are reported for the two hours immediately following injection and vigilance states were not differentiated. Periodograms were generated based on vigilance states of slow-wave sleep (non-rapid eye

Author Manuscript Author Manuscript Author Manuscript Author Manuscript

movement; NREM), paradoxical sleep (REM), and wake which were determined by delta power, theta power, muscle tone, and movement. The value of each parameter for each vigilance state are as follows: NREM: mid-high delta power, low-mid theta power, low-mid muscle tone, low movement; REM: low delta power, high theta power, low muscle tone, low movement; wake: low-mid delta power, low-high theta power, high muscle tone, low-high movement. Periodograms were generated in 10 s epochs to obtain relative percent power for each of the following frequency bands within each vigilance state: delta 0.5–4 Hz, theta 4–8 Hz, alpha 8–12 Hz, sigma 12–16 Hz, beta 16–24 Hz, and gamma 25–40 Hz. The total average (of 720 10-s epochs) percent power is reported. Data reflect EEG spikes and spectral density patterns during a consecutive two-hour period immediately following injection.

2.5. Tissue collection (Study 3)

Mice were euthanized 1–3 h following the final injection. Mice were anesthetized using isoflurane prior to cervical dislocation. The chest cavity was opened using sharp scissors and a 27-gauge needle was inserted into the left ventricle. The inferior vena cava was severed, and mice were saline perfused by hand using a syringe filled with ~15 ml PBS. Mice were decapitated using sharp scissors, the brain removed and bisected into right and left hemispheres using a razor blade. The left hemisphere was micro-dissected to collect hippocampus, cortex and cerebellum tissue. These tissues were flash-frozen on dry ice and stored at − 80 °C until prepared for western blotting. The right hemisphere was post-fixed in 10% formalin for 24 h, immersed in 30% sucrose until sunk, rinsed and stored in PBS at 4 °C until sectioning and histological staining.

2.6. Western blotting (Study 3)

Cortical and hippocampal tissue lysates were prepared by using a plastic pestle to hand homogenize frozen tissue in 100 μL Pierce RIPA lysis buffer (Thermo Scientific, Cat # 89901) with cOmplete EDTA-free protease inhibitor cocktail (Roche, 04693132001). Lysates were spun down at 10,000 *g* for 5 min and supernatant transferred to a new tube. Protein concentration was measured by a standard bicinchoninic acid (BCA) assay protocol (Pierce BCA Protein Assay Kit, Thermo Scientific). Samples were denatured with NuPage LDS sample buffer (Thermo Scientific, cat # NP0007) and reducing agent (Thermo Scientific, cat # NP0009) and 10 μg protein was loaded on Bolt™ 4–12% Bis-Tris Plus gels (Thermo Scientific, cat # NW04120BOX). Gels were run at 200 V for 30 min and gel transfer performed using the iBlot2™ system on to nitrocellulose membranes (Thermo Scientific, cat # IB23001). Following transfer, gels were rehydrated in DI water overnight and Coomassie stained (Bio-Rad, cat # 161–0786) for 60 min for use as a loading control. Membranes were blocked in 5% nonfat milk in TBST for 60 min prior to incubation with primary antibodies overnight. Each blot was probed a total of three times; blots were stripped (Restore™ Western Blot Stripping Buffer, Thermo Scientific, cat # VA293256) and re-blocked between probes. Proteins were probed in the following order: Glutamate Transporter 1 (GLT1) at 1:4000 (Millipore Sigma, AB1783), Excitatory Amino Acid Transporter 1 (EAAT1/GLAST) at 1:1000 (Novus Biologicals, NB100–1869) and glial fibrillary acidic protein (GFAP) at 1:5000 (Millipore Sigma, MAB360). Secondary antibodies were HRP conjugated anti-guinea, anti-rabbit, or anti-mouse IgG (Promega, W402B) diluted at 1:10,000 in 5% nonfat milk in TBST. A subset of hippocampal

Author Manuscript Author Manuscript Author Manuscript Author Manuscript

lysates were first boiled (95° water bath for 3 min) and 30 μg protein was loaded per well. These nitrocellulose membranes were probed for pro- and cleaved-caspase 3 (Novus Biologicals, 31A1067) at 1:2000 in 5% milk in PBST. Protein bands were detected using chemiluminescence (Perkin Elmer, Western Lightning Plus-ECL, cat # NEL104001EA) and analyzed with ImageJ (imagej.nih.gov). Values reported represent each individual protein normalized to total protein as a loading control (Coomassie stained gel) and to the average WT saline expression for each blot. Cortical and hippocampal tissue were run on separate gels and thus expression levels between tissue type cannot be directly compared.

Histology *(Study 3)* – Frozen sections (35 μm thick) were cut from the formalin-fixed hemibrain using a benchtop sliding microtome (Leica). Sections were floated in 24-well plates containing 1xPBS and then mounted on gelatin-coated, charged glass microscope slides. Three to five sections spaced approximately 100 μm apart were used per mouse for quantification of Aβ plaques between (sagittal sections, 1–2.5 mm lateral (Paxinos and Franklin, 2001)). Aβ was stained with Thioflavin-S (1%, Sigma Aldrich, USA) for 5 min following dehydration in 70% ethanol. Digital images of the hippocampus and overlying cortex were taken using a fluorescent imaging microscope (EVOSfl, AMGmicro) at a magnification of 4×. Area occupied by Aβ plaques was determined using the freely-available Image J software (National Institute of Health, Bethesda, MD, USA). Quantification was performed by an experienced researcher who was blind to the treatment of the mice. Some WT sections were also stained as negative controls, but only sections from APP/PSEN1 mice were quantified. Plaques were counted and coverage was calculated as percent of total region measured, in pixels.

2.7. Statistics

Data are reported in figures and text as Mean +/− S.E.M. unless otherwise stated.—Data were analyzed using SPSS 26.0 or GraphPad Prism version 6 or higher. Data were first checked for normality, skew and outliers that may reflect experimental or software error and removed if outside of 95% confidence interval. Data reflecting expected variability in behavioral data were not removed. Where necessary, data were analyzed using non-parametric analyses as described in results. All analyses were first run with sex as a fixed variable. There were no significant meaningful differences according to sex, thus all data were collapsed and analyzed together. Univariate ANOVA (2 genotype × 2 treatment) was conducted for tests with single dependent variables. Behavioral tests with multiple trials were analyzed with Repeated Measures (RM)- ANOVAs with the same between-groups factors as above. For study 3, EEG spike and spike train data were not normally distributed between treatments and therefore were analyzed separately by treatment based on a priori predictions that KA would increase number of EEG spikes and spike trains (i.e., main effect of treatment) whereas few, if any, spikes and spike trains were anticipated in saline-treated WT mice.

Author Manuscript Author Manuscript Author Manuscript Author Manuscript

3. Results

3.1. Study 1

In study 1 we investigated the differential effects of KA on hippocampal LTP in WT and young APP/PSEN1 mice, with the hypothesis that APP/PSEN1 mice would be more affected by this treatment even if differences were not present at baseline in these young animals. Input-output curves for each group were performed for both the relationship between stimulation intensity and both presynaptic fiber volley and slope of the field EPSP (Fig. 1B). The fiber volley/EPSP slope ratio was also similar between groups (Fs < 2.326, Ps > 0.142, Fig.1 Biii). No differences were noted between experimental groups suggesting no treatment or genotypic difference in axonal excitability or synaptic strength. In response to 5 days of treatment with 5 mg/kg KA (Fig. 1A) WT mice showed a decrease in the post-tetanic potentiation period (PTP, 27.2 ± 6.6%) but normal appearing late-phase LTP (99.8 ± 1.1% vs 87.4 ± 2.8% in saline treated)(Fig. 1C), as might be expected due to the high intensity TBS protocol used (Kang-Park et al., 2003). A similar pattern of blunted PTP was observed in APP/PSEN1 mice receiving saline (17.4 ± 4.3% $n = 8$), suggesting that these changes may be related to alterations in presynaptic release of glutamate or potentially post-synaptic clearance due to the acute KA injection. The saline-treated APP/PSEN1 mice had normal LTP at this age (99.1 ± 1.1% $n = 7$), which is consistent with the literature (Trinchese et al., 2004). However, in the APP/PSEN1 mice receiving KA hippocampal LTP was significantly impaired (38.7 ± 0.6%, $p < 0.0001$ tukey post-hoc), suggesting potential impairments in post-synaptic glutamate clearance and highlighting the increased sensitivity to the drug in those mice (Fig. 1C–E).

3.2. Study 2

In Study 2 we tested the hypothesis that repeated induced hyperexcitability from low-dose KA would impact learning and memory in APP/PSEN1 mice to a greater extent than in WT littermates. We used young mice in which Aβ accumulation and deposition are low in order to test these effects independent of heavy Aβ plaque load. WT and APP/PSEN1 mice were treated with 7.5–10 mg/kg KA or the vehicle saline twice per week beginning at 12 weeks of age (Fig. 2A).

3.2.1. Survival—Four separate cohorts of mice were utilized for behavioral testing. This permitted behavioral testing to be completed within 4-h time blocks to limit potential effects of circadian rhythms on data, particularly because greater seizure activity was noted during the dark cycle. The first three cohorts of mice were treated with 10 mg/kg KA which led to significantly greater mortality in the APP/PSEN1-KA mice than in any of the other groups (Gehan-Breslow-Wilcoxon test $c^2 = 33.75$, $P < 0.0001$, Fig. 2B). Notably these mice typically died in the time period (3–4 days) between the two KA injections and not as an immediate result of the injection itself. Mice were found dead following the active period at night and it is presumed that they died from seizures, although this was not actively observed. Therefore, for the fourth cohort of mice KA concentration was decreased to 7.5 mg/kg to facilitate survival of enough APP/PSEN1 mice to complete behavioral testing. Of the 2 WT-SAL, 4 WT-KA, 2 APP/PSEN1-SAL and 4 APP/PSEN1-KA in cohort 4, only

Author Manuscript Author Manuscript Author Manuscript Author Manuscript

one mouse died during the modified (7.5 mg/kg) treatment schedule, an APP/PSEN1 mouse following the second KA treatment.

3.2.2. Behavior—Data are presented for all surviving mice for each task. Approximately equal numbers of male and female mice were randomized into treatment and control groups and all surviving mice were utilized in behavioral testing. Data are combined for all groups of mice including both concentrations of KA and final group numbers are presented in below. Data are combined for all groups of mice including both concentrations of KA and final group numbers were WT-SAL 7 male, 8 female, WT-KA 6 male, 8 female, APP/PSEN1-SAL 7 male, 2 Female, APP/PSEN1-KA 3 male, 7 female. Some mice died prior to completion of all tasks therefore N for the APP/PSEN1-KA group is lower for tasks that were conducted at the end of the behavioral battery.

3.2.3. Elevated zero maze—There were no differences in exploration of closed versus open zones of the maze indicating that neither genotype nor treatment impact anxiety in a novel behavioral task in these mice (Genotype $F_{1, 44} = 0.878$, $P = 0.354$, Treatment $F_{1, 44} = 0.410$, $P = 0.525$, Interaction $F_{1, 44} = 0.078$, $P = 0.781$, Fig. 2C). Although APP/PSEN1 mice showed a slight tendency to explore further during the 5-min EZM session there was no effect of KA treatment (Genotype $F_{1, 44} = 7.007$, $P = 0.011$, Treatment $F_{1, 44} = 0.20$, $P = 0.657$, Interaction $F_{1, 44} = 0.264$, $P = 0.610$, Fig. 2D).

3.2.4. Locomotor activity—Baseline locomotor activity across 30 min in activity chambers was similar across all groups regardless of genotype or treatment (Genotype $F_{1, 42} = 0.020$, $P = 0.889$, Treatment $F_{1, 42} = 0.260$, $P = 0.613$, Interaction $F_{1, 42} = 0.759$, $P = 0.388$, Fig. 2E).

3.2.5. Two trial Y-maze—Memory for the two previous explored arms was indicated by a preference for the novel arm compared to the familiar arms. All groups showed a preference for the novel arm (WT-SAL $t(11) = 5.640$, $P < 0.001$; APP/PSEN1-SAL $t(10) = 3.308$, $P = 0.008$; WT-KA $t(13) = 2.761$, $P = 0.016$, APP/PSEN1-KA $t(9) = 2.613$, $P = 0.028$, Fig. 2F). Percent of time spent in the novel arm did not vary among groups (Fs1, 47 < 0.882, Ps > 0.353).

3.2.6. Morris water maze—Mice were first trained on the visible platform version of the task to ensure that rule learning (find the platform to escape maze) was intact, and mice were physically able to perform the task, Fig. 2G,H. All mice learned to locate the platform in the different quadrants across the 2 days of training (Day $F_{1, 43)} = 142.583$, $P < 0.001$). Overall the fastest escape latencies were observed in the APP/PSEN1-KA-treated animals although this difference was not significant ($F_{1, 43} = 4.034$, $P = 0.051$) with no other differences according to genotype or treatment (Fs < 1.035, Ps > 0.315). Mice were then trained for 5 days to locate a hidden platform that remained in the same location. All groups showed decreasing escape latencies over time ($F_{4, 172} = 27.590$, $P < 0.001$) with no differences among groups (Fs < 1.324, Ps > 0.263, Fig. 2I). During the probe trial learning was assessed via preferential swimming in the target quadrant versus the non-target quadrants. All groups showed evidence of a preferential search pattern (WT-SAL $F_{3, 36} = 41.545$, $P < 0.001$; APP/PSEN1 SAL $F_{3, 36} = 13.385$, $P < 0.001$; WT-KA $F_{3, 27} = 18.206$, P

Author Manuscript Author Manuscript Author Manuscript Author Manuscript

< 0.001, APP/PSEN1-KA $F_{3, 27} = 25.586$, $P < 0.001$, Fig. 2J). No differences were observed in total swim path length (Fs < 0.535, Ps > 0.468) or time spent in the perimeter (Fs < 1.283, Ps > 0.264).

We have previously shown that young APP/PSEN1 mice are still able to perform this task well, even following a single KA injection (10 mg/kg), but are impaired when task demands are increased through moving the platform location (reversal learning (Mi et al., 2018)). All mice were able to acquire the new platform location ($F_{2, 84} = 38.912$, P < 0.001) with no differences observed among groups (Fs < 0.769, Ps > 0.386, Fig. 2K). However, recall of the platform location during the probe trial was impaired in the APP/PSEN1-KA-treated animals only (preference for platform quadrant (WT-SAL $F_{3, 36} = 10.162$, P < 0.001; APP/PSEN1-SAL $F_{3, 27} = 4.846$, $P = 0.008$; WT-KA $F_{3, 39} = 8.151$, P < 0.001, APP/PSEN1-KA $F_{3, 24} = 25.551$, $P < 0.079$, Fig. 2L). There were no group differences in perimeter swim time (Fs < 0.169, Ps > 0.683), distance traveled (Fs < 1.317, Ps > 0.258) or swim speed (Fs < 1.363, Ps > 0.250).

3.2.7. Force plate actimeters—Force plate actimeters were used to provide an automated measurement of activity and immobility time during the first 20 min following administration of KA. Data are not included for cohort 1 (WT-saline $N = 4$, APP/PSEN saline $N = 3$, WT-KA N = 4, APP/PSEN1 KA $N = 2$) due to a technical error during data acquisition meaning that raw data files were not saved. Greater bouts of immobility (time spent immobile during a 5-s time bin) were observed in KA-treated mice than in saline-treated animals (treatment $F_{1, 28} = 18.445$, $P < 0.001$), with the greatest immobility observed in KA-treated APP/PSEN1 mice (genotype $F_{1, 28} = 2.985$, $P = 0.095$; interaction $F_{1, 28} = 5.472$, $P = 0.027$, Fig. 2M,N). Data were collapsed into 5-min time bins and compared between genotypes in KA-treated mice only. Both WT and APP/PSEN1 mice appeared to have recovered from acute effects of injection with return to normal activity levels by 20 min post treatment, and the largest differences between the two groups were noted between 5- and 15-min post injection (Time $F_{3, 48} = 20.640$, P < 0.001; Genotype $F_{1, 16} = 6.089$, $P = 0.025$; Interaction $F_{3, 48} = 3.679$, $P = 0.018$).

3.3. Study 3

The dramatic mortality observed in young APP/PSEN1 mice treated with 10 mg/kg KA suggested that even this low concentration was having long-term effects on neuronal signaling in the mice. Deaths were not an immediate effect of treatments, and occurred up to 3 days following injection, suggesting a kindling effect so we also sought to identify the potentially long-term nature of changes that arose from KA treatment. Therefore, we fitted 14-week-old mice of both sexes and genotypes with implantable telemetry devices to measure changes in EEG signaling in freely moving mice in response to repeated low-dose KA treatment (Fig. 3A). Since our aim was to assess consequences from subclinical abnormal epileptiform activity following repeated subthreshold activation of the glutamatergic system, two mice (one female APP/PSEN1 and one female WT) were omitted from all analyses due to frank tonic-clonic seizures following KA injection. Two additional male APP/PSEN1-KA treated mice died midway through the study, one was confirmed as

Author Manuscript Author Manuscript Author Manuscript Author Manuscript

a result of a KA-induced seizure, and EEG data collected during week 1 of the study was removed from EEG analyses.

3.3.1. Spikes and spike train activity—Example traces for normal activity, spike trains and spikes are shown in Fig. 3Bi–iii. Among saline-treated mice, we observed increased spiking activity in APP/PSEN1 compared to WT which remained consistently higher over the four-week duration of the study (Genotype $F_{1, 12} = 5.479$, $P = 0.037$, Test Week $F_{1, 12} = 0.100$, $P = 0.921$; Fig. 3C). There was an average of 43.75 ± 27.07 and 41.75 ± 27.07 spikes detected in the two-hour period following injection in WT-SAL treated mice during weeks 1 and 4 of the study, respectively, a frequency of electrographic spikes considered normal in WT-SAL mice on C57Bl/6 J background (Purtell et al., 2018). A greater number of spikes were observed in APP/PSEN1-SAL treated mice during the same two-hour period in weeks 1 and 4 with an average of 86.00 ± 54.30 and 89.17 ± 40.65 spikes, respectively (mean ± SD). Spike trains were not detected in WT-SAL treated mice whereas APP/PSEN1-SAL mice exhibited a low number of spontaneous spike trains throughout the recording period (week 1, 5.17 ± 4.708; week 4, 3.83 ± 3.48)(Genotype $F_{1, 12} = 9.99$, $P = 0.009$, Test Week $F_{1, 12} = 1.132$, $P = 0.273$)(Fig. 3D).

KA increased overall spike activity comparably in both genotypes (Treatment $F_{1, 26} = 5.834$, $P = 0.023$), with no significant cumulative changes between weeks 1 (after the first treatment) and 4 (after the seventh treatment) (Genotype $F_{1, 26} = 0.447$, $P = 0.510$, Test Week $F_{1, 26} = 3.740$, $P = 0.064$, all interaction Ps > 0.05). WT-KA treated mice had an average of 257.36 ± 475.14 spikes in week 1 and 416.45 ± 709.83 spikes in week 4 and APP/PSEN1-KA treated mice had an average of 200.00 ± 173.68 and 765.60 ± 860.96 spikes in weeks 1 and 4, respectively (Fig. 3C). However, KA treatment affected spike train activity in WT and APP/PSEN1 groups differently throughout the four-week recording period (Genotype $F_{1, 26} = 4.590$, $P = 0.042$, Treatment $F_{1, 26} = 7.100$, $P = 0.013$, Test Week $F_{1, 26} = 3.442$, $P = 0.075$, 3-way Interaction $F_{1, 26} = 4.788$, $P = 0.046$). WT-KA treated mice had 7.36 ± 18.19 spike trains in week 1 with 6.55 ± 15.48 in week 4 whereas KA increased spike trains by roughly 3-fold in APP/PSEN1 mice from week 1 (10.2 ± 12.518) to week 4 of recording (35 ± 34.32) (Fig. 3D). Baseline spikes and spike train activity were analyzed for all animals with available data ($n = 20$ of 30 animals) and we confirmed that within a genotype there were no significant differences between assigned treatment groups prior to first injection (both Ps > 0.05) (Supplemental Fig. 2).

3.3.2. Power band analyses—Rather than only focus on the individual spikes recorded we also analyzed the data by parsing it into functionally distinct power bands of differing frequency ranges. Average percent power across 6 EEG frequency bands (delta, theta, alpha, sigma, beta and gamma) was computed for the two hours immediately following injections during weeks 1 and 4. Data were first categorized according to behavioral state including sleep (REM and non-REM, NREM; Fig. 3E). There were no significant differences in spectral power over time (all Ps > 0.05) suggesting that any effects of KA on spike activity or cognitive changes is unlikely to be simply a reflection of altered behavioral states (Fig. 3Fi–iii; week 4 data only shown for brevity). During wake periods, percent sigma (Genotype $F_{1, 26} = 15.54$, $P = 0.0005$), beta (Genotype $F_{1, 26} = 24.09$, $P < 0.0001$),

Author Manuscript Author Manuscript Author Manuscript Author Manuscript

and gamma (Genotype $F_{1, 26} = 11.04$, $P = 0.0027$) power were significantly increased in APP/PSEN1 compared to WT mice with no main effects of KA (all Treatment Ps > 0.05). During NREM sleep, percent alpha (Genotype $F_{1, 26} = 4.526$, $P = 0.0430$,), sigma (Genotype $F_{1, 26} = 5.757$, $P = 0.0239$), and beta (Genotype $F_{1, 26} = 11.02$, P = 0.0027) power were significantly increased in APP/PSEN1 compared to WT mice. During REM sleep, percent theta (Genotype $F_{1, 26} = 8.543$) power was significantly decreased and percent beta (Genotype $F_{1, 26} = 18.03$, $P = 0.0003$) power was significantly increased in APP/PSEN1 compared to WT mice with no main effects of KA (all Treatment Ps > 0.05). During REM periods, gamma power was affected by KA differentially in each genotype (Genotype $F_{1, 26} = 4.907$, $P = 0.0365$, Treatment $F_{1, 26} = 0.8049$, $P = 0.3786$, Interaction $_{F1, 26} = 5.898$, $P = 0.0230$). KA increased gamma power in WT mice, but not in APP/PSEN1 mice, in which higher percent gamma power was already observed.

3.3.3. Locomotor activity—Similar to the assessment in Study 2, locomotor activity was comparable across all groups regardless of genotype or treatment in Study 3 (Genotype $F_{1, 26} = 0.775$ $P = 0.387$, Treatment $F_{1, 26} = 2.337$, $P = 0.135$, Interaction $F_{1, 26} = 0.787$, $P = 0.383$) (Fig. 4A).

3.3.4. Elevated zero maze—APP/PSEN1 mice in Study 3 showed the same modest tendency to explore further based on total distance traveled during the 5-min EZM session as those in Study 2, but there was no effect of KA treatment (Genotype $F_{1, 26} = 4.941$, $P = 0.035$, Treatment $F_{1, 26} = 0.385$, $P = 0.541$, Interaction $F_{1, 26} = 0.132$, $P = 0.712$) (Fig. 4B). Neither genotype nor treatment impacted anxiety in a novel behavioral task in these mice measured by time spent in the closed zones of the apparatus (Genotype $F_{1, 26} = 0.110$, $P = 0.743$, Treatment $F_{1, 26} = 0.012$, $P = 0.914$, Interaction $F_{1, 26} = 0.102$, $P = 0.752$) (Fig. 4C).

3.3.5. Contextual fear conditioning—During training, prior to administration of the tone-shock pairing, APP/PSEN1 mice displayed an increase in baseline freezing behavior compared to WT with no impact of treatment (Genotype $F_{1, 26} = 7.88$, $P = 0.009$, Treatment $F_{1, 26} = 0.451$, $P = 0.508$, Interaction $F_{1, 26} = 0.037$, $P = 0.850$, *data not shown*). Appropriate contextual memory retrieval was observed in all genotype-treatment groups approximately 24 h later when placed in the same context without the tone-shock pairing, supported by a significant increase in freezing time from baseline to testing trial with no differences between genotypes or treatment (Trial $F_{1, 26} = 275.962$, $P < 0.0001$, Genotype $F_{1, 26} = 3.408$, $P = 0.076$, Treatment $F_{1, 26} = 0.530$, $P = 0.473$, all Interaction Ps > 0.05). Post-hoc paired *t*-tests confirm that each individual genotype-treatment group spent a significantly greater length of time freezing during the testing trial compared to baseline (Ps < 0.01, Fig. 4D).

3.3.6. Cued fear conditioning—Memory retrieval of the shock-associated cue was assessed one hour following contextual memory retrieval. All groups spent significantly greater time freezing following onset of the shock-associated cue compared to time spent freezing when first introduced to the novel context (Trial $F_{1, 26} = 109.017$, P <0.0001). However, the same increase in freezing behavior in response to the cue was not observed uniformly in all groups (Genotype $F_{1, 26} = 6.404$, $P = 0.018$, Treatment $F_{1, 26} = 5.190$, $P = 0.031$; Genotype*Trial Interaction $F_{1, 26} = 7.55$, $P = 0.011$). APP/PSEN1-KA mice

Author Manuscript Author Manuscript Author Manuscript Author Manuscript

spent more time freezing overall compared to WT in both the novel context and during the presentation of the shock-associated cue and did not exhibit differential freezing between the two parts of the trial ($P = 0.149$). Memory of the tone-shock pairing was evident in all other mice through increased freezing during the tone (Post-hoc paired t-tests Ps < 0.01) (Fig. 4E).

3.3.7. Glutamate transport proteins

3.3.7.1. Cortex.: APP/PSEN1-SAL mice exhibit decreased GLT-1 protein expression in cortical tissue compared to WT controls, and KA lowered expression in both genotypes (Genotype $F_{1, 26} = 10.49$, $P = 0.003$, Treatment $F_{1, 26} = 19.07$, $P < 0.001$, Interaction $F_{1, 26} = 0.017$, $P = 0.897$; Fig. 4F,I). There were no main effects of genotype nor treatment on cortical GLAST expression (Genotype $F_{1, 26} = 0.269$, $P = 0.610$, Treatment $F_{1, 26} = 0.693$, $P = 0.413$). A significant interaction among the factors (Interaction $F_{1, 26} = 6.436$, P = 0.018) was not supported by significant follow-up analyses (Fig. 4G,I). GFAP expression was similar among all groups suggesting a lack of gliosis in APP/PSEN1 mice at this age or in response to repeated KA (Genotype $F_{1, 26} = 1.714$, $P = 0.202$, Treatment $F_{1, 26} = 1.604$, $P = 0.217$, Interaction $F_{1, 26} = 0.022$, $P = 0.883$, Fig. 4H,I).

3.3.7.2. Hippocampus.: Hippocampal GLT-1 expression was not significantly different between APP/PSEN1- and WT-SAL treated mice. KA decreased hippocampal GLT-1 expression only in APP/PSEN1 mice (Genotype $F_{1, 26} = 0.051$, $P = 0.823$, Treatment $F_{1, 26} = 6.66$, $P = 0.016$, Interaction $F_{1, 26} = 7.231$, $P = 0.005$, Fig. 4J). Overall lower GLAST expression was observed in APP/PSEN1 mice at baseline and there was no significant effect of KA on GLAST expression in the hippocampus of either genotype (Genotype $F_{1, 26} = 4.476$, $P = 0.044$, Treatment $F_{1, 26} = 3.162$, $P = 0.087$, Interaction $F_{1, 26} = 0.058$, $P = 0.811$, Fig. 4K). Similar to results in cortical tissue, there was no evidence of gliosis in the hippocampus regardless of genotype or treatment (GFAP: Genotype $F_{1, 26} = 0.742$, $P = 0.397$, Treatment $F_{1, 26} = 0.821$, $P = 0.373$, Interaction $F_{1, 26} = 0.626$, $P = 0.423$, Fig. 4L). A marker of apoptosis was measured by western blot in the hippocampus of a subset of animals and under these conditions KA did not alter pro-caspase-3 (Genotype $F_{1,19} = 0.038$, $P = 0.847$, Treatment $F_{1, 19} = 0.171$, $P = 0.684$, Interaction $F_{1, 19} = 0.026$, $P = 0.874$) nor cleaved-caspase-3 (Genotype $F_{1,19} = 0.857$, $P = 0.366$, Treatment $F_{1, 19} = 0.0006$, $P = 0.980$, Interaction $F_{1, 19} \leq 0.0001$, $P = 0.999$) expression in either genotype (*data not shown*).

3.3.7.3. Histology.: Aβ-coverage, as observed through staining with Thioflavin-S was sparse in hippocampus of all APP/PSEN1 mice. The maximum number of Aβ-deposits observed in a single section was five, and many animals had no observable plaques in hippocampus (*data not shown*).

4. Discussion

We demonstrated that short-term (daily for 5 days) and long-term repeated (twice per week for up to 16 weeks) treatment with a low dose of the kainite receptor agonist kainic acid (KA) was sufficient to disrupt LTP, to cause mild memory deficits in high-cognitive demand behavioral tasks, exacerbate the modest abnormal epileptiform activity present in APP/PSEN1 mice and uniquely affect expression of glutamatergic clearance proteins. It is

Author Manuscript Author Manuscript Author Manuscript Author Manuscript

particularly notable that these modifications occurred in young APP/PSEN1 mice, less than 6 months old. Furthermore, the study had higher-than-expected mortality rates indicating that the data available for analysis was from the least impacted animals. Aβ-plaques are not observed or are extremely sparse in APP/PSEN1 mice at this age, thus these findings suggest that potential contributions to cognitive decline from hyperexcitability in AD occur independent of heavy Aβ-plaque load. Nevertheless, even young APP/PSEN1 mice generate and accumulate Aβ monomers and larger oligomers from 2 months or even earlier (Dixit et al., 2017), and the same sensitivity to KA was not observed in WT mice. Therefore, although this process may be a very early facet of AD pathobiology and not dependent on presence of heavy plaque load, it is not necessarily independent from oligomeric Aβ nor APP overexpression.

A growing body of research suggests that hyperexcitability and subclinical or manifest epilepsy may be a critical part of AD pathology and strongly linked to cognitive decline. Seizures occur much more frequently in AD patients compared to other dementia patients (Vossel et al., 2017). Subclinical epileptiform activity also occurs in a substantial number of AD patients, with recent studies using long-term EEG monitoring showing between 42 and 52% of AD patients with non-convulsive seizures or epileptiform discharges (Horvath et al., 2018; Vossel et al., 2016). AD patients with epilepsy may have an earlier diagnosis and more severe cognitive status (Cumbo and Ligori, 2010; Rauramaa et al., 2018) and treating with anti-seizure medications may improve cognition, even in cases of mild cognitive impairment (Bakker et al., 2015; Cumbo and Ligori, 2010). Multiple transgenic mouse lines for Aβ-expression and AD also exhibit spontaneous seizures and increased sensitivity to evoked seizures (Minkeviciene et al., 2009; Vogt et al., 2011) but it is not known how this sensitivity may impact the cognitive impairments observed. Not only can Aβ affect neuronal activity but increased synaptic activity by hippocampal perforant pathway stimulation in young (3–5 month) Tg2576 mice has been shown to increase interstitial Aβ levels (Cirrito et al., 2005). Similarly, experimentally-induced hyperactivity has also been shown to increase Aβ load in 9–14-month old 3 × Tg mice treated with pilocarpine to induce epilepsy (Yan et al., 2012). We did not observe increase in mature compact Aβ plaques stained by Thioflavin-S staining in our KA-treated APP/PSEN1 mice in the current study. Nevertheless, it is likely that, particularly as mice age and Aβ pathology accelerates, there is a positive-feedback relationship between hyperexcitability and Aβ load.

A heterogeneous group of cortical spike discharge types was recorded in young (4.5–6 month) APP/PSEN1 mice – some present in both genotypes and some cortical spikes unique to APP/PSEN1 mice (including ‘giant spikes’), but were not observed in all individual animals (Gureviciene et al., 2019). The giant spikes which implicate synchronous hippocampal and cortical epileptic signals were associated with increased likelihood of convulsive seizures. The association of hippocampal dysfunction with greatest seizure activity is a likely explanation for the marginal cognitive deficits observed in our study since APP/PSEN1 mice that suffered active seizures (observed through EEG or presumed as cause of death) were not included in analyses due to attrition (Studies 2 and 3) or removal (Study 3). The different patterns of spike activity, including giant spikes, may thus be an important feature for inclusion in future studies.

Author Manuscript Author Manuscript Author Manuscript Author Manuscript

Epilepsy itself is often accompanied by cognitive deficits (Elger et al., 2004). These deficits are present in both acquired and genetic mouse models of epilepsy (Cheah et al., 2012; Kim et al., 2020), with corresponding deficits in hippocampal plasticity (Kullmann et al., 2000). Chemoconvulsants including KA are typically used in preclinical epilepsy models to induce overt seizures or status epilepticus, with accompanying cell death and significant pathology (Levesque and Avoli, 2013). Immediately after such acute seizure events, before there is significant pathology, hippocampal LTP may be immediately preserved or enhanced, while with time it becomes severely attenuated (Zhang et al., 2010). Thus, in the absence of potential damaging cytotoxic effects of seizures, short-term low dose systemic KA would be expected to have little detrimental effect on plasticity, similar to our results in KA-treated WT mice. Mice that are resistant to KA-induced status epilepticus may have enhanced, rather than impaired hippocampal plasticity (Suarez et al., 2012). Hippocampal neuronal apoptosis has indeed been prevented by a pre-conditioning exposure to controlled electroconvulsive shocks prior to KA-induced status epilepticus (Kondratyev et al., 2001), suggesting the possibility that repeated exposure to low-dose KA may induce similar protective changes. We did not detect apoptosis under the conditions in Study 3 using western blot to measure activated caspase-3 (*data not shown*), however, we do not discount the possibility entirely because apoptosis could have been specific to a subregion of the hippocampus. Over a longer period of time repeated epileptiform discharges and seizures in the hippocampus contribute to functional and structural disruption, excitotoxic cell death, and ultimately impaired LTP and memory functions that are observed in those animals that go on to have spontaneous seizures (Groticke et al., 2008). This latter case better represents the impaired LTP observed in the APP/PSEN1 mice treated with KA in the current study.

Several genetic mouse models of AD evaluated report normal SC-CA1 LTP at early ages (<3 months)(Marchetti and Marie, 2011) including in APP/PSEN1 mice (Calella et al., 2010; Trinchese et al., 2004) with impaired LTP not witnessed until much later time points when Aβ pathology is more established (Calella et al., 2010; Gengler et al., 2010; Trinchese et al., 2004). In contrast in 3xTg mice, basal transmission, paired-pulse facilitation, and LTP were all normal compared to wild-types up to 14 months of age suggesting that accumulating Aβ is not sufficient for impaired LTP (Fitzjohn et al., 2010). Modest differences in the baseline slopes (Fig. 1) suggest some mild disruption of LTP in APP/PSEN1 mice even at 12 weeks, but we only observed significantly impaired LTP in KA-treated APP/PSEN1.

Our study differs from previous work in this area in that we were able to make extended behavioral and EEG measurements in the APP/PSEN1 mice across a long-term treatment schedule. The EEG measurements in freely moving (non-tethered) mice within their home cages also increases the validity of findings since it does not increase stress or anxiety in the mice through needing to be tethered to recording equipment in unfamiliar cage set ups during data acquisition. We showed modest changes in number of spikes observed in KA-treated APP/PSEN1 mice and a greater increase in the numbers of spike trains (at least 3 spikes recorded together). There were genotype differences in the relative ratio of five of the six power bands analyzed (theta, alpha, sigma, beta, and gamma) dependent on vigilance state and only gamma waves were also further affected by KA in WT mice. Elevations in alpha, beta and gamma waves may be indicative of a combination of attention and anxiety, and the increases observed in the young APP/PSEN1 may reflect increased

Author Manuscript Author Manuscript Author Manuscript Author Manuscript

effort required for higher order cognitive processing. During the brief two-hour period analyzed, we do not report altered sleep patterns in APP/PSEN1 mice or by KA treatment, indicated by comparable time spent in each vigilance state among genotype-treatment groups. Nevertheless, during REM sleep we report decreased theta power in APP/PSEN1 mice in the current study. These findings are consistent with other studies reporting lower theta and delta power observed in 8–10 month old APP/PSEN1 mice although frank sleep patterns were unaltered (Kent et al., 2018), whereas other studies report sleep-wake cycle disruption and diurnal variations in APP/PSEN1 mice with onset of plaque deposition from 6 to 9 months of age (Roh et al., 2012). In the present study, APP/PSEN1 mice show increased alpha, sigma, and beta power during NREM sleep. Increased sigma power during NREM sleep has previously been positively correlated with interictal spike rate in patients with drug-resistant focal epilepsy (Zubler et al., 2017) and increased sigma and beta during NREM are reported in individuals suffering from insomnia (Spiegelhalder et al., 2012). In sum, the changes shown here are in mice younger than are typically studied and reflect the potential for increased sensitivity to further disruption, such as may be caused by KA or other forms of excitotoxic signaling.

Altered glutamatergic signaling is the major related neuropathological difference tying together AD and epilepsy. Addition of Aβ to WT mouse astrocytes in culture significantly decreased GLT-1 surface expression (Scimemi et al., 2013). GLT-1 is the most abundant glutamate transporter in the brain represents approximately 80% of glutamate transporters in the hippocampus (Lehre and Danbolt, 1998). Thus, its dysfunction may be linked to hippocampal-dependent memory deficits. Poorer recall was observed in the Morris water maze in APP/PSEN1 mice lacking one allele for GLT-1 (Mookherjee et al., 2011; Tanaka et al., 1997). Changes in glutamatergic genes or gene levels have been reported in clinical post mortem tissue (Kirvell et al., 2006; Masliah et al., 1996) as well as in mouse models of AD (Minkeviciene et al., 2008; Schallier et al., 2011), although transporters, methods and even brain areas often vary between studies precluding direct comparison. We observed clear decreases in GLT-1 expression in cortical tissue from APP/PSEN1-saline control mice even at less than 6 months with little Aβ accumulation. Repeated low-dose KA treatment further decreased GLT-1 expression in cortex of both WT and APP/PSEN1 animals. This finding suggests that the same pathways impacted by KA administration may already be disrupted in the transgenic mice. The cortical GLT-1 protein expression findings coincide with our EEG spike findings; KA-treatment makes the WT behave similarly to saline-treated APP/PSEN1 mice and KA induces abnormal activity in both genotypes. In slight contrast to this result we found no baseline differences in hippocampal GLT-1 between WT and APP/PSEN1, but a significant decrease in expression following KA treatments in APP/PSEN1 mice only. These protein expression findings align with our data showing intact LTP in saline-treated APP/PSEN1 mice but significant impairments only in APP/PSEN1 mice treated acutely with KA. GLAST expression was modestly decreased in APP/PSEN1 mice in hippocampus only and GFAP expression was unchanged in either tissue suggesting a relatively discrete effect on GLT-1. Overall, these findings fit well with the behavioral data that showed normal cognition under baseline conditions in these young APP/PSEN1 animals, but early memory deficits in KA-treated mice under cognitively demanding tasks that are reliant on hippocampal function. That we see differences in electrophysiological

Author Manuscript Author Manuscript Author Manuscript Author Manuscript

and behavioral measures in response to KA in APP/PSEN1, as well as protein expression changes, suggests that these underlie the functional changes observed although we do not discount the potential role other neurotransmitter systems may play in AD pathology. Microglial and inflammatory processes also contribute to AD-related neuronal dysfunction and altered glutamatergic signaling. Rats with the p.R47H variant in the microglial gene *Trem2* exhibited increased glutamate transmission associated with increased TNF-α and not Aβ (Ren et al., 2020).

At the age studied here (<6 months), APP/PSEN1 mice do not show robust cognitive deficits (Dixit et al., 2015; Mi et al., 2018; Reiserer et al., 2007). Indeed, even APP/PSEN1-KA-treated animals were able to perform most of the tasks presented appropriately. It was only in the most challenging of behavioral tasks used, namely platform placement during reversal learning in the Morris water maze, and the cued-trial during conditioned fear testing, that this group exhibited a deficit. Mice that were most sensitive to KA died during testing and thus to detect differences in the least affected remaining mice suggests that this could be a greater issue in cases with less cognitive reserve. We propose that to induce any deficit in young APP/PSEN1 mice that typically perform at a WT-equivalent level is quite important. We hypothesize that this is likely due to KA treatment exacerbating at least one facet of the neuropathology associated with the APP/PSEN1 genotype, which may be a combination of APP dysregulation or oligomeric Aβ generation but not heavy Aβ plaque load. It is particularly important for Alzheimer's disease research that such modest changes in EEG signaling may be associated with any memory deficit at all, suggesting that hyperexcitability may need to be a very early target in order to protect against memory loss.

5. Conclusions

If these data can be directly translated to human cases then it is possible that some of the cognitive decline observed in AD and perhaps MCI patients are due to hyperexcitability and undetected, subclinical or subthreshold seizure activity rather than directly linked to other AD pathologies. Since neurotransmitter changes are more tractable to pharmacological manipulation, this may provide increased opportunity to modify or slow decline regardless of accumulating neuropathology. EEG is a method that is directly translatable to human populations which may also provide an additional early diagnostic marker to identify patients that might most benefit from interventions.

Supplementary Material

Refer to Web version on PubMed Central for supplementary material.

Acknowledgements

This material is based upon work supported by the Department of Veterans Affairs, Veterans Health Administration, Office of Research and Development, (VA Merit Review I01 CX001610 to JMM). JW is supported by the Vanderbilt Interdisciplinary Training Program in Alzheimer's Disease (T32 AG058524). RB is supported by the Vanderbilt Training Program in Environmental Toxicology (T32 ES007028). We would like to acknowledge the support of Carlo Malabanan in the Vanderbilt Mouse Metabolic Phenotyping Center (MMPC) who performed all of the EEG surgeries for this study. WN is supported by American Epilepsy Society (Junior Investigator Award), a pilot grant from the National Institute for Neurologic Disease and Stroke's Center for SUDEP Research (CSR), and the Vanderbilt Faculty Research Scholars award. All behavioral studies were performed in the Vanderbilt Mouse

Author Manuscript Author Manuscript Author Manuscript Author Manuscript

Neurobehavioral laboratory which receives support from the Vanderbilt Kennedy Center (P50 HD103537). The MMPC is supported by (U2C DK059637).

Abbreviations:

KA	kainic acid
SAL	saline
IP	intraperitoneal
LTP	long term potentiation
PTP	post tetanic potentiation
Aβ	beta-amyloid
WT	wild-type
APP/PSEN1	amyloid precursor protein / presenilin 1
EEG	electroencephalogram
FPA	force plate actimeters
BLM	bouts of low mobility
REM	rapid eye movement
NREM	non rapid eye movement

References

Bakker A, Albert MS, Krauss G, et al., 2015. Response of the medial temporal lobe network in amnestic mild cognitive impairment to therapeutic intervention assessed by fMRI and memory task performance. Neuroimage Clin. 7, 688–698 (PMC4377841). [PubMed: 25844322]

Calella AM, Farinelli M, Nuvolone M, et al., 2010. Prion protein and Abeta-related synaptic toxicity impairment. EMBO Mol. Med. 2 (8), 306–314 (PMC2962809). [PubMed: 20665634]

Cavus I, Kasoff WS, Cassaday MP, et al., 2005. Extracellular metabolites in the cortex and hippocampus of epileptic patients. Ann. Neurol. 57 (2), 226–235. [PubMed: 15668975]

Cheah CS, Yu FH, Westenbroek RE, et al., 2012. Specific deletion of NaV1.1 sodium channels in inhibitory interneurons causes seizures and premature death in a mouse model of Dravet syndrome. Proc. Natl. Acad. Sci. U. S. A109 (36), 14646–14651 (PMC3437823). [PubMed: 22908258]

Chin J, Scharfman HE, 2013. Shared cognitive and behavioral impairments in epilepsy and Alzheimer's disease and potential underlying mechanisms. Epilepsy Behav. 26 (3), 343–351. [PubMed: 23321057]

Cirrito JR, Yamada KA, Finn MB, et al., 2005. Synaptic activity regulates interstitial fluid amyloid-beta levels in vivo. Neuron48 (6), 913–922. [PubMed: 16364896]

Cretin B, Philippi N, Bousiges O, et al., 2017a. Do we know how to diagnose epilepsy early in Alzheimer's disease?Rev. Neurol. 173 (6), 374–380. [PubMed: 28501143]

Cretin B, Philippi N, Dibitonto L, et al., 2017b. Epilepsy at the prodromal stages of neurodegenerative diseases. Geriatr. Psychol. Neuropsychiatr. Vieil. 15 (1), 75–82. [PubMed: 28266344]

Cumbo E, Ligori LD, 2010. Levetiracetam, lamotrigine, and phenobarbital in patients with epileptic seizures and Alzheimer's disease. Epilepsy Behav. 17 (4), 461–466. [PubMed: 20188634]

Author Manuscript Author Manuscript Author Manuscript Author Manuscript

Danbolt NC, Storm-Mathisen J, Kanner BI, 1992. An [Na+ + K+]coupled L-glutamate transporter purified from rat brain is located in glial cell processes. Neuroscience51 (2), 295–310. [PubMed: 1465194]

Dixit S, Bernardo A, Walker JM, et al., 2015. Vitamin C deficiency in the brain impairs cognition, increases amyloid accumulation and deposition, and oxidative stress in APP/PSEN1 and normally aging mice. ACS Chem. Neurosci. 6 (4), 570–581 (PMC4476071). [PubMed: 25642732]

Dixit S, Fessel JP, Harrison FE, 2017. Mitochondrial dysfunction in the APP/PSEN1 mouse model of Alzheimer's disease and a novel protective role for ascorbate. Free Rad. Biol. Med. 112, 515–523 (PMC5623070). [PubMed: 28863942]

Elger CE, Helmstaedter C, Kurthen M, 2004. Chronic epilepsy and cognition. Lancet Neurol. 3 (11), 663–672. [PubMed: 15488459]

Fitzjohn SM, Kuenzi F, Morton RA, et al., 2010. A study of long-term potentiation in transgenic mice over-expressing mutant forms of both amyloid precursor protein and presenilin-1. Mol. Brain3 (1), 21 (PMC2912307). [PubMed: 20630068]

Gengler S, Hamilton A, Holscher C, 2010. Synaptic plasticity in the hippocampus of a APP/PS1 mouse model of Alzheimer's disease is impaired in old but not young mice. PLoS One5 (3), e9764 (PMC2842299). [PubMed: 20339537]

Groticke I, Hoffmann K, Loscher W, 2008. Behavioral alterations in a mouse model of temporal lobe epilepsy induced by intrahippocampal injection of kainate. Exp. Neurol. 213 (1), 71–83. [PubMed: 18585709]

Gureviciene I, Ishchenko I, Ziyatdinova S, et al., 2019. Characterization of epileptic spiking associated with brain amyloidosis in APP/PS1 mice. Front. Neurol. 10, 1151 (PMC6861424). [PubMed: 31781019]

Gurevicius K, Lipponen A, Tanila H, 2013. Increased cortical and thalamic excitability in freely moving APPswe/PS1dE9 mice modeling epileptic activity associated with Alzheimer's disease. Cereb. Cortex23 (5), 1148–1158. [PubMed: 22581851]

Horvath A, Szucs A, Barcs G, et al., 2016. Epileptic seizures in Alzheimer disease: a review. Alzheimer Dis. Assoc. Disord. 30 (2), 186–192. [PubMed: 26756385]

Horvath A, Szucs A, Hidasi Z, et al., 2018. Prevalence, semiology, and risk factors of epilepsy in Alzheimer's disease: an ambulatory EEG study. J. Alzheimers Dis. 63 (3), 1045–1054. [PubMed: 29710705]

Jen JC, Wan J, Palos TP, et al., 2005. Mutation in the glutamate transporter EAAT1 causes episodic ataxia, hemiplegia, and seizures. Neurology65 (4), 529–534. [PubMed: 16116111]

Joutsa J, Rinne JO, Hermann B, et al., 2017. Association between childhood-onset epilepsy and amyloid burden 5 decades later. JAMA Neurol. 74 (5), 583–590 (PMC5822199). [PubMed: 28346588]

Kang-Park MH, Sarda MA, Jones KH, et al., 2003. Protein phosphatases mediate depotentiation induced by high-intensity theta-burst stimulation. J. Neurophysiol. 89 (2), 684–690. [PubMed: 12574446]

Kent BA, Strittmatter SM, Nygaard HB, 2018. Sleep and EEG power spectral analysis in three transgenic mouse models of Alzheimer's disease: APP/PS1, 3xTgAD, and Tg2576. J. Alzheimers Dis. 64 (4), 1325–1336 (PMC6176720). [PubMed: 29991134]

Kim HK, Gschwind T, Nguyen TM, et al., 2020. Optogenetic intervention of seizures improves spatial memory in a mouse model of chronic temporal lobe epilepsy. Epilepsia61 (3), 561–571. [PubMed: 32072628]

Kirvell SL, Esiri M, Francis PT, 2006. Down-regulation of vesicular glutamate transporters precedes cell loss and pathology in Alzheimer's disease. J. Neurochem. 98 (3), 939–950. [PubMed: 16893425]

Kondratyev A, Sahibzada N, Gale K, 2001. Electroconvulsive shock exposure prevents neuronal apoptosis after kainic acid-evoked status epilepticus. Brain Res. Mol. Brain Res. 91 (1–2), 1–13. [PubMed: 11457487]

Kullmann DM, Asztely F, Walker MC, 2000. The role of mammalian ionotropic receptors in synaptic plasticity: LTP, LTD and epilepsy. Cell. Mol. Life Sci. 57 (11), 1551–1561. [PubMed: 11092450]

Author Manuscript Author Manuscript Author Manuscript Author Manuscript

Lam AD, Deck G, Goldman A, et al., 2017. Silent hippocampal seizures and spikes identified by foramen ovale electrodes in Alzheimer's disease. Nat. Med. 23 (6), 678–680. [PubMed: 28459436]

Lehre KP, Danbolt NC, 1998. The number of glutamate transporter subtype molecules at glutamatergic synapses: chemical and stereological quantification in young adult rat brain. J. Neurosci. 18 (21), 8751–8757. [PubMed: 9786982]

Levesque M, Avoli M, 2013. The kainic acid model of temporal lobe epilepsy. Neurosci. Biobehav. Rev. 37 (10 Pt 2), 2887–2899 (PMC4878897). [PubMed: 24184743]

Losing P, Niturad CE, Harrer M, et al., 2017. SRF modulates seizure occurrence, activity induced gene transcription and hippocampal circuit reorganization in the mouse pilocarpine epilepsy model. Mol. Brain10 (1), 30 (PMC5513048). [PubMed: 28716058]

Marchetti C, Marie H, 2011. Hippocampal synaptic plasticity in Alzheimer's disease: what have we learned so far from transgenic models?Rev. Neurosci. 22 (4), 373–402. [PubMed: 21732714]

Masliah E, Alford M, DeTeresa R, et al., 1996. Deficient glutamate transport is associated with neurodegeneration in Alzheimer's disease. Ann. Neurol. 40 (5), 759–766. [PubMed: 8957017]

McCarson KE, Winter MK, Abrahamson DR, et al., 2018. Assessing complex movement behaviors in rodent models of neurological disorders. Neurobiol. Learn. Mem. 165, 106817. [PubMed: 29476821]

McNair LF, Andersen JV, Aldana BI, et al., 2019. Deletion of neuronal GLT-1 in mice reveals its role in synaptic glutamate homeostasis and mitochondrial function. J. Neurosci. 39 (25), 4847–4863 (PMC6670249). [PubMed: 30926746]

Mi DJ, Dixit S, Warner TA, et al., 2018. Altered glutamate clearance in ascorbate deficient mice increases seizure susceptibility and contributes to cognitive impairment in APP/PSEN1 mice. Neurobiol. Aging71, 241–254 (PMC6162152). [PubMed: 30172223]

Minkeviciene R, Ihalainen J, Malm T, et al., 2008. Age-related decrease in stimulated glutamate release and vesicular glutamate transporters in APP/PS1 transgenic and wild-type mice. J. Neurochem. 105 (3), 584–594. [PubMed: 18042177]

Minkeviciene R, Rheims S, Dobszay MB, et al., 2009. Amyloid beta-induced neuronal hyperexcitability triggers progressive epilepsy. J. Neurosci. 29 (11), 3453–3462. [PubMed: 19295151]

Mookherjee P, Green PS, Watson GS, et al., 2011. GLT-1 loss accelerates cognitive deficit onset in an Alzheimer's disease animal model. J. Alzheimers Dis. 26 (3), 447–455 (PMC3256092). [PubMed: 21677376]

Pajarillo E, Rizor A, Lee J, et al., 2019. The role of astrocytic glutamate transporters GLT-1 and GLAST in neurological disorders: potential targets for neurotherapeutics. Neuropharmacology161, 107559 (PMC6731169). [PubMed: 30851309]

Palop JJ, Chin J, Roberson ED, et al., 2007. Aberrant excitatory neuronal activity and compensatory remodeling of inhibitory hippocampal circuits in mouse models of Alzheimer's disease. Neuron55 (5), 697–711. [PubMed: 17785178]

Paxinos G, Franklin KBJ, 2001. The Mouse Brain in Stereotaxic Coordinates, 2nd ed. Academic, San Diego, CA.

Petr GT, Sun Y, Frederick NM, et al., 2015. Conditional deletion of the glutamate transporter GLT-1 reveals that astrocytic GLT-1 protects against fatal epilepsy while neuronal GLT-1 contributes significantly to glutamate uptake into synaptosomes. J. Neurosci. 35 (13), 5187–5201 (PMC4380995). [PubMed: 25834045]

Purtell H, Dhamne SC, Gurnani S, et al., 2018. Electrographic spikes are common in wild-type mice. Epilepsy Behav. 89, 94–98 (PMC7325561). [PubMed: 30399547]

Rauramaa T, Saxlin A, Lohvansuu K, et al., 2018. Epilepsy in neuropathologically verified Alzheimer's disease. Seizure58, 9–12. [PubMed: 29602145]

Reiserer RS, Harrison FE, Syverud DC, et al., 2007. Impaired spatial learning in the APPSwe + PSEN1DeltaE9 bigenic mouse model of Alzheimer's disease. Genes Brain Behav. 6 (1), 54–65. [PubMed: 17233641]

Ren S, Yao W, Tambini MD, et al., 2020. Microglia TREM2(R47H) Alzheimer-linked variant enhances excitatory transmission and reduces LTP via increased TNF-alpha levels. Elife9, PMC7338048.

Author Manuscript Author Manuscript Author Manuscript Author Manuscript

Roberson ED, Halabisky B, Yoo JW, et al., 2011. Amyloid-beta/Fyn-induced synaptic, network, and cognitive impairments depend on tau levels in multiple mouse models of Alzheimer's disease. J. Neurosci. 31 (2), 700–711 (PMC3325794). [PubMed: 21228179]

Roh JH, Huang Y, Bero AW, et al., 2012. Disruption of the sleep-wake cycle and diurnal fluctuation of beta-amyloid in mice with Alzheimer's disease pathology. Sci. Transl. Med4 (150), 150ra22 (PMC3654377).

Schallier A, Smolders I, Van Dam D, et al., 2011. Region- and age-specific changes in glutamate transport in the AbetaPP23 mouse model for Alzheimer's disease. J. Alzheimers Dis. 24 (2), 287–300. [PubMed: 21297271]

Scimemi A, Meabon JS, Woltjer RL, et al., 2013. Amyloid-beta1–42 slows clearance of synaptically released glutamate by mislocalizing astrocytic GLT-1. J. Neurosci. 33 (12), 5312–5318 (3866500). [PubMed: 23516295]

Sharma A, Kazim SF, Larson CS, et al., 2019. Divergent roles of astrocytic versus neuronal EAAT2 deficiency on cognition and overlap with aging and Alzheimer's molecular signatures. Proc. Natl. Acad. Sci. U. S. A116 (43), 21800–21811 (PMC6815169). [PubMed: 31591195]

Spiegelhalder K, Regen W, Feige B, et al., 2012. Increased EEG sigma and beta power during NREM sleep in primary insomnia. Biol. Psychol. 91 (3), 329–333. [PubMed: 22960269]

Suarez LM, Cid E, Gal B, et al., 2012. Systemic injection of kainic acid differently affects LTP magnitude depending on its epileptogenic efficiency. PLoS One7 (10), e48128 (PMC3485282). [PubMed: 23118939]

Takahashi K, Kong Q, Lin Y, et al., 2015. Restored glial glutamate transporter EAAT2 function as a potential therapeutic approach for Alzheimer's disease. J. Exp. Med. 212 (3), 319–332 (PMC4354363). [PubMed: 25711212]

Tanaka K, Watase K, Manabe T, et al., 1997. Epilepsy and exacerbation of brain injury in mice lacking the glutamate transporter GLT-1. Science (New York, NY)276 (5319), 1699–1702.

Trinchese F, Liu S, Battaglia F, et al., 2004. Progressive age-related development of Alzheimer-like pathology in APP/PS1 mice. Ann. Neurol. 55 (6), 801–814. [PubMed: 15174014]

Vogt DL, Thomas D, Galvan V, et al., 2011. Abnormal neuronal networks and seizure susceptibility in mice overexpressing the APP intracellular domain. Neurobiol. Aging32 (9), 1725–1729 (PMC2889215). [PubMed: 19828212]

Volicer L, Smith S, Volicer BJ, 1995. Effect of seizures on progression of dementia of the Alzheimer type. Dementia6 (5), 258–263. [PubMed: 8528372]

Vossel KA, Beagle AJ, Rabinovici GD, et al., 2013. Seizures and epileptiform activity in the early stages of Alzheimer disease. JAMA Neurol. 70 (9), 1158–1166 (4013391). [PubMed: 23835471]

Vossel KA, Ranasinghe KG, Beagle AJ, et al., 2016. Incidence and impact of subclinical epileptiform activity in Alzheimer's disease. Ann. Neurol. 80 (6), 858–870. [PubMed: 27696483]

Vossel KA, Tartaglia MC, Nygaard HB, et al., 2017. Epileptic activity in Alzheimer's disease: causes and clinical relevance. Lancet Neurol. 16 (4), 311–322 (PMC5973551). [PubMed: 28327340]

Yan XX, Cai Y, Shelton J, et al., 2012. Chronic temporal lobe epilepsy is associated with enhanced Alzheimer-like neuropathology in 3xTg-AD mice. PLoS One7 (11), e48782 (3498246). [PubMed: 23155407]

Zhang Y, Cai GE, Yang Q, et al., 2010. Time-dependent changes in learning ability and induction of long-term potentiation in the lithium-pilocarpine-induced epileptic mouse model. Epilepsy Behav. 17 (4), 448–454. [PubMed: 20332069]

Ziyatdinova S, Ronnback A, Gurevicius K, et al., 2016. Increased Epileptiform EEG activity and decreased seizure threshold in Arctic APP transgenic mouse model of Alzheimer's disease. Curr. Alzheimer Res. 13 (7), 817–830. [PubMed: 26825094]

Zubler F, Rubino A, Lo Russo G, et al., 2017. Correlating interictal spikes with sigma and Delta dynamics during non-rapid-eye-movement-sleep. Front. Neurol. 8, 288 (PMC5479894). [PubMed: 28690583]

Author Manuscript Author Manuscript Author Manuscript Author Manuscript

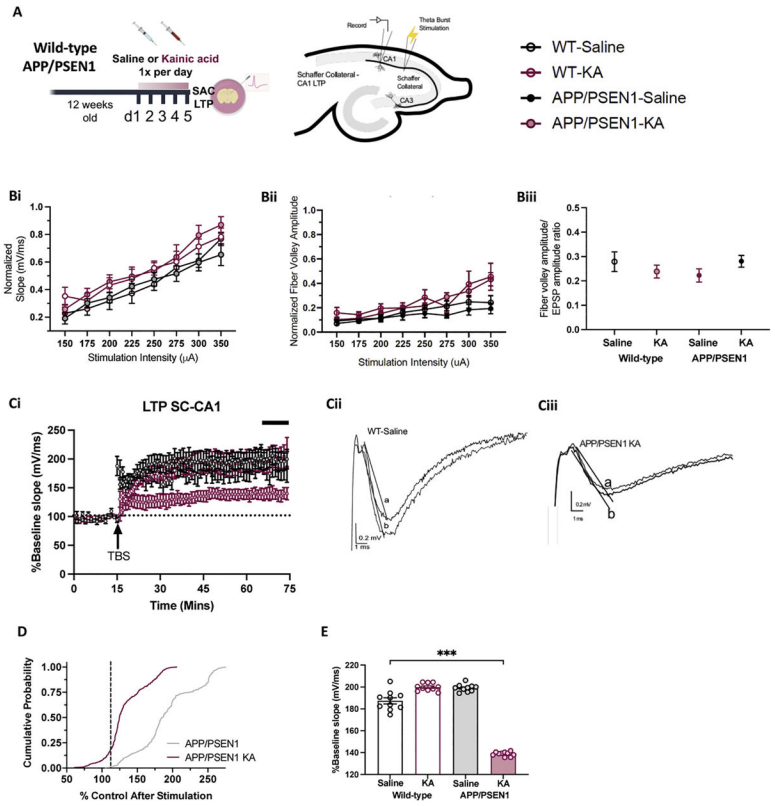

Fig. 1.

APP/PSEN1 mice are more sensitive to the effects of kainic acid on long term potentiation (LTP). (A) Timeline for experimental treatments and illustration of Field potential (fEPSP) recorded in acute horizontal hippocampal slices. (B) Input-output curves for each group were performed for the relationship between stimulation intensity and both (Bi) presynaptic fiber volley and (Bii) slope of the field EPSP and (Biii) fiber volley//EPSP ratio at experimental stimulus intensity. (C) Theta-burst stimulation (TBS) at SC-CA1 induced enhanced LTP in WT (Ci) and APP/PSEN1 (Cii) animals treated with saline or KA over 5 days, recorded at 0.05 Hz. Representative traces at baseline (point a) and 55 mins post induction (point b) for WT control and KA-treated APP/PSEN1 animals (Ciii). (D) Cumulative probability of post-TBS normalized slopes from individual experiments in APP/PSEN1 animals. (E) Pooled potentiation at 55–60 min. Post-TBS. Late LTP analyses indicate a dramatic decrease in APP/PSEN1-KA ($P < 0.001$ compared to all other groups). Data show mean +/− S.E.M. *, *** $P < 0.05$, 0.001 as marked.

Author Manuscript Author Manuscript Author Manuscript Author Manuscript

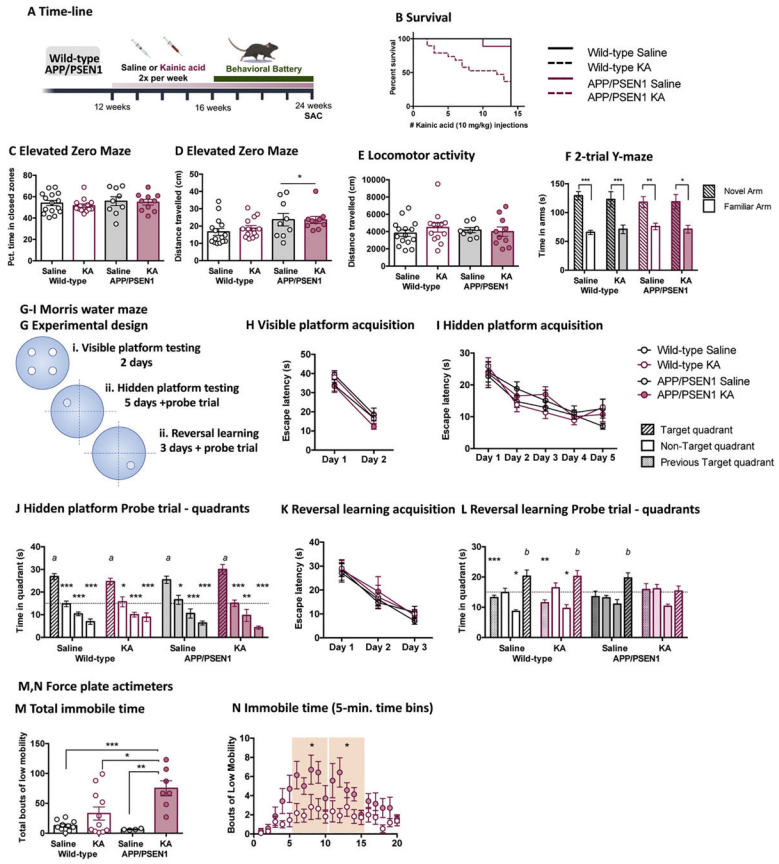

Fig. 2.

APP/PSEN1 mice are more sensitive to the effects of repeated low-dose kainic acid on learning and memory. (A) Timeline of experiments. (B) Survival curve for all genotypes treated with kainic acid (KA) (7.5–10 mg/kg) twice per week. Young APP/PSEN1 mice treated with KA showed (C) normal anxiety in the elevated zero maze. (D) Exploration in the zero maze was slightly greater in APP/PSEN1 mice but all groups were within expected ranges. No genotype or treatment effects were observed in (E) locomotor activity in a novel environment, or (F) working memory in the two-trial Y-maze task. (G) All mice were trained on the visible platform version of the water maze, followed by 5 days of hidden platform training, a probe trial to test 24-h recall, and re-training to a new platform location (reversal learning). All mice were able to acquire (H) the visible platform task and (I) learn the location of the hidden platform as shown by decreasing escape latencies across test sessions. (J) 24-h recall was not affected by genotype or treatment and all mice showed a preference for the quadrant that had contained the platform. (K) Mice were also able to learn a new location of the platform, however, (L) KA-treated APP/PSEN1 showed no preference for the target quadrant during the 24 h recall probe test. (M,N) KA increased time spent immobile in both genotypes following final KA treatment although this was observed to a greater extent in APP/PSEN1 mice than WT. *, **, *** $P < 0.05, 0.01, 0.001$ as marked (D, F, M, N) or compared to the target quadrant (J, L). Pairwise comparisons following significant omnibus ANOVA or interactions. (J, L) [a, b,] $P < 0.001, 0.05$ compared to chance performance (by one sample t-test compared to 15 s, indicated by dotted line. WT SAL

Author Manuscript Author Manuscript Author Manuscript Author Manuscript

t(12) = 2.553, P = 0.025, WT-KA t(13) = 2.692, P = 0.018, APP-SAL t(9) = 4.70, P = 0.021, APP-KA = t(8) = 0.211, P = 0.838). Surviving animals included in study 2 analyses were 8 male and 8 female WT-SAL, 6 male and 8 female WT-KA, 7 male and 2 female APP/PSEN1-SAL, 3 male and 7 female APP/PSEN1-KA.

Author Manuscript Author Manuscript Author Manuscript Author Manuscript

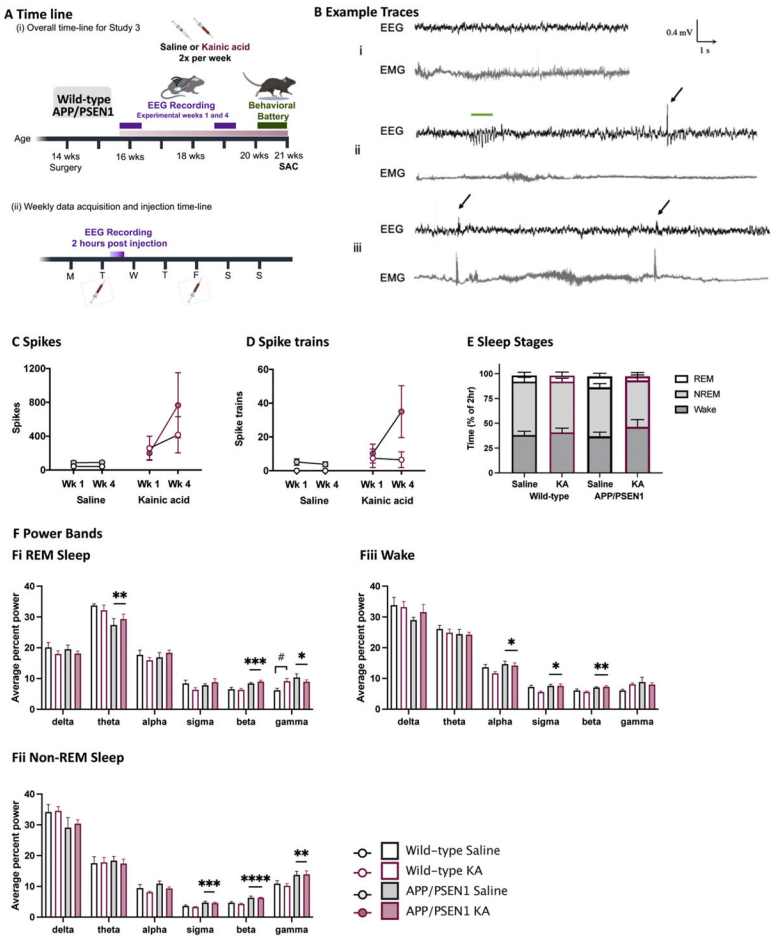

Fig. 3.

Abnormal EEG patterns are detected in young APP/PSEN1 mice and are exacerbated by repeated low-dose kainic acid. (A) Timeline of treatment and experiments. (B) Example traces shown for EEG (black, upper traces) and EMG (gray, lower traces). (Bi) Normal EEG signal in a resting but awake mouse. (Bii) Example of a spike train (green bar above EEG) associated with a behavioral pause (EMG), followed by a 750 uv amplitude single spike (arrow). (Biii) Spikes (arrows) characteristic during visually confirmed (by synchronized video) head bobbing show increased EMG (neck muscle) activity. (C) Total number of spikes detected two hours post injection during weeks 1 and 4 of EEG recordings. (D) Total number of spike trains detected two hours post injection during weeks 1 and 4 of EEG recordings. (E) Data for 2-h post-KA parsed according to wake state (Awake, REM, and NREM sleep). (F) Average percent power contributed by each of 6 frequency domains in each of the four genotype and treatment groups during week 4 recording only during awake, REM sleep and non-REM sleep. Average power of all frequencies except delta differed according to genotype in at least one behavioral state. Delta 0.5–4 Hz, theta 4–8 Hz, alpha 8–12 Hz, sigma 12–16 Hz, beta 16–24 Hz, and gamma 25–40 Hz frequencies. *, **, *** $P < 0.05, 0.01, 0.001$ main effect of genotype (F). # $P < 0.05$ significant effect of KA treatment, post hoc pairwise comparison as marked.

Author Manuscript Author Manuscript Author Manuscript Author Manuscript

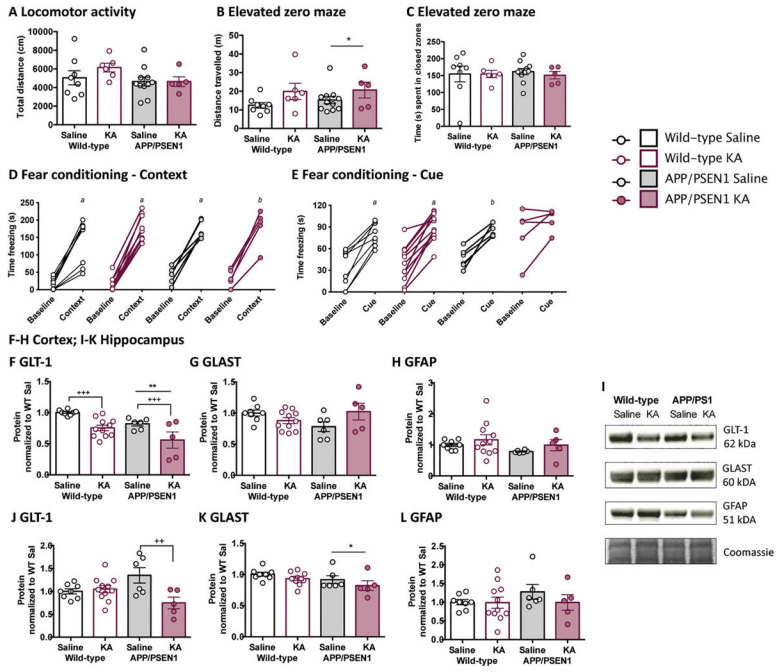

Fig. 4.

Altered memory and expression of glutamate transporters in APP/PSEN1 and kainic acid treated mice. (A) Total locomotor activity (distance traveled over 60 min) did not differ between genotypes and was not affected by treatment. (B) APP/PSEN1 mice show a subtle tendency to explore more (travel a greater distance) in a 5 min elevated zero maze task but (C) time spent in the closed zone of the elevated zero maze, and thus anxiety levels during a novel behavioral task, were comparable among all groups. (D) All four experimental groups display appropriate context memory retrieval and (E) all groups except for APP/PSEN1-KA mice exhibit cue-associated memory retrieval. (F) Cortical GLT-1, (G) GLAST, and (H) GFAP protein expression. (I) Representative blot images are the same samples (cortex) on the same blot but stripped between probes, with total protein loaded (Coomassie Blue stain). Hippocampal (J) GLT-1, (K) GLAST, and (L) GFAP protein expression. Surviving animals included in study 3 analyses were 4 male and 4 female WT-SAL, 5 male and 6 female WT-KA, 3 male and 3 female APP/PSEN1-SAL, 2 male and 3 female APP/PSEN1-KA. *, ** $P < 0.05$, 0.01 main effect of genotype (B,F,K). $^{a, b,}$ $P < 0.001$, 0.01 compared to baseline or novel context performance (by one sample t-test, D,E). $^{+, ++, +++}$ $P < 0.05$, 0.01, main effect or post hoc pairwise comparison effect of KA treatment (F,J).